Design of a Paclitaxel Prodrug Conjugate for Active Targeting of an Enzyme Upregulated in Breast Cancer Cells

ARTICLE *in* MOLECULAR PHARMACEUTICS · MAY 2014

Impact Factor: 4.38 · DOI: 10.1021/mp500128k · Source: PubMed

5 AUTHORS, INCLUDING:

Ratna Vadlamudi
University of Texas Health Science Center at S…
182 PUBLICATIONS **6,569** CITATIONS
SEE PROFILE

Joo L Ong
University of Texas at San Antonio
156 PUBLICATIONS **5,086** CITATIONS
SEE PROFILE

molecular pharmaceutics

Article

pubs.acs.org/molecularpharmaceutics

Design of a Paclitaxel Prodrug Conjugate for Active Targeting of an Enzyme Upregulated in Breast Cancer Cells

Arpan Satsangi,*[,†,‡] Sudipa S. Roy,[§] Rajiv K. Satsangi,[∥] Ratna K. Vadlamudi,[§] and Joo L. Ong[‡]

[†]Joint Graduate Program in Biomedical Engineering, University of Texas at San Antonio and the University of Texas Health Science Center at San Antonio, San Antonio, Texas 78249, United States

[‡]Department of Biomedical Engineering, University of Texas at San Antonio, San Antonio, Texas 78249, United States

[§]Department of Obstetrics and Gynecology, University of Texas Health Science Center at San Antonio San Antonio, Texas78229, United States

[∥]RANN Research Corporation, San Antonio, Texas 78250, United States

ABSTRACT: Breast cancer is the second most common cause of cancer-related deaths in women. Chemotherapy is an important treatment modality, and paclitaxel (PTX) is often the first-line therapy for its metastatic form. The two most notable limitations related to PTX-based treatment are the poor hydrophilicity of the drug and the systemic toxicity due to the drug's nonspecific and indiscriminate distribution among the tissues. The present work describes an approach to counter both challenges by designing a conjugate of PTX with a hydrophilic macromolecule that is coupled through a biocleavable linker, thereby allowing for active targeting to an enzyme significantly upregulated in cancer cells. The resultant strategy would allow for the release of the active ingredient preferentially at the site of action in related cancer cells and spare normal tissue. Thus, PTX was conjugated to the hydrophilic poly(amdioamine) [PAMAM] dendrimer through the cathepsin B-cleavable tetrapeptide Gly-Phe-Leu-Gly. The PTX prodrug conjugate (PGD) was compared to unbound PTX through *in vitro* evaluations against breast cancer cells and normal kidney cells as well as through *in vivo* evaluations using xenograft mice models. As compared to PTX, PGD demonstrated a higher cytotoxicity specific to cell lines with moderate-to-high cathepsin B activity; cells with comparatively lower cathepsin B activity demonstrated an inverse of this relationship. Regression analysis between the magnitude of PGD-induced cytotoxic increase over PTX and cathepsin B expression showed a strong, statistically significant correlation ($r^2 = 0.652$, $p < 0.05$). The PGD conjugate also demonstrated a markedly higher tumor reduction as compared to PTX treatment alone in MDA-MB-231 tumor xenograft models, with PGD-treated tumor volumes being 48% and 34% smaller than PTX-treated volumes at weeks 2 and 3 after treatment initiation.

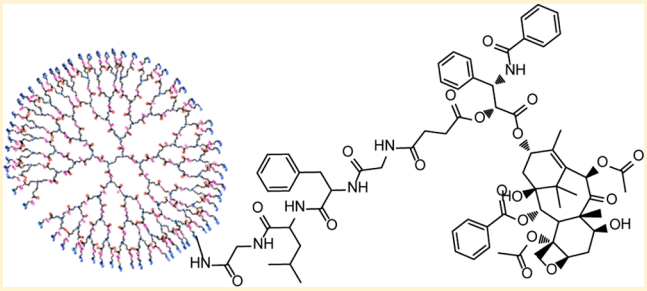

KEYWORDS: *paclitaxel−dendrimer conjugate, active targeting, biocleavable linker, cathepsin B, breast cancer, drug delivery*

INTRODUCTION

Breast cancer accounts for the second largest number of cancer deaths in the United States, with more than 230,000 new cases diagnosed every year.[1,2] While chemotherapy plays a central role in cancer treatment, common anticancer agents demonstrate well-known limitations, including systemic toxicity, poor solubility in body fluids, and slow tumor uptake among other pharmacological barriers. Recent nanotechnological advancements are being applied to overcome these problems. This research is one such effort toward targeted delivery and improved efficacy of an anticancer agent commonly used for the treatment of breast cancer.

The broadly cytotoxic class of drugs taxanes, including paclitaxel (PTX) and docetaxel, is the most effective single-agent drug used in breast cancer therapy and is considered the first-line therapy in metastatic form of the disease.[3,4] Among taxanes, PTX is used more preferentially[5] as the response rate of PTX in patients with metastatic breast cancer has been confirmed to be 56%.[6,7] Therefore, PTX was chosen as a model anticancer drug against the breast cancer cells in this study.

Anticancer treatment involving PTX faces several limitations. The most notable challenge is its poor aqueous solubility and the slow dissolution rate in bodily fluids. PTX is a diterpenoid centered on a bulky and complex taxane ring with a number of hydrophobic substituents. It lacks ionizable functional groups, which otherwise would have allowed for possible solubilization with moderation in pH and formation of salts and charged complexes. These characteristics render the molecule a log *P* value of about 3.96 and an aqueous solubility of less than 0.01

Received: February 12, 2014
Revised: April 30, 2014
Accepted: May 6, 2014
Published: May 21, 2014

Scheme 1. Synthesis of the Paclitaxel−GFLG Conjugate

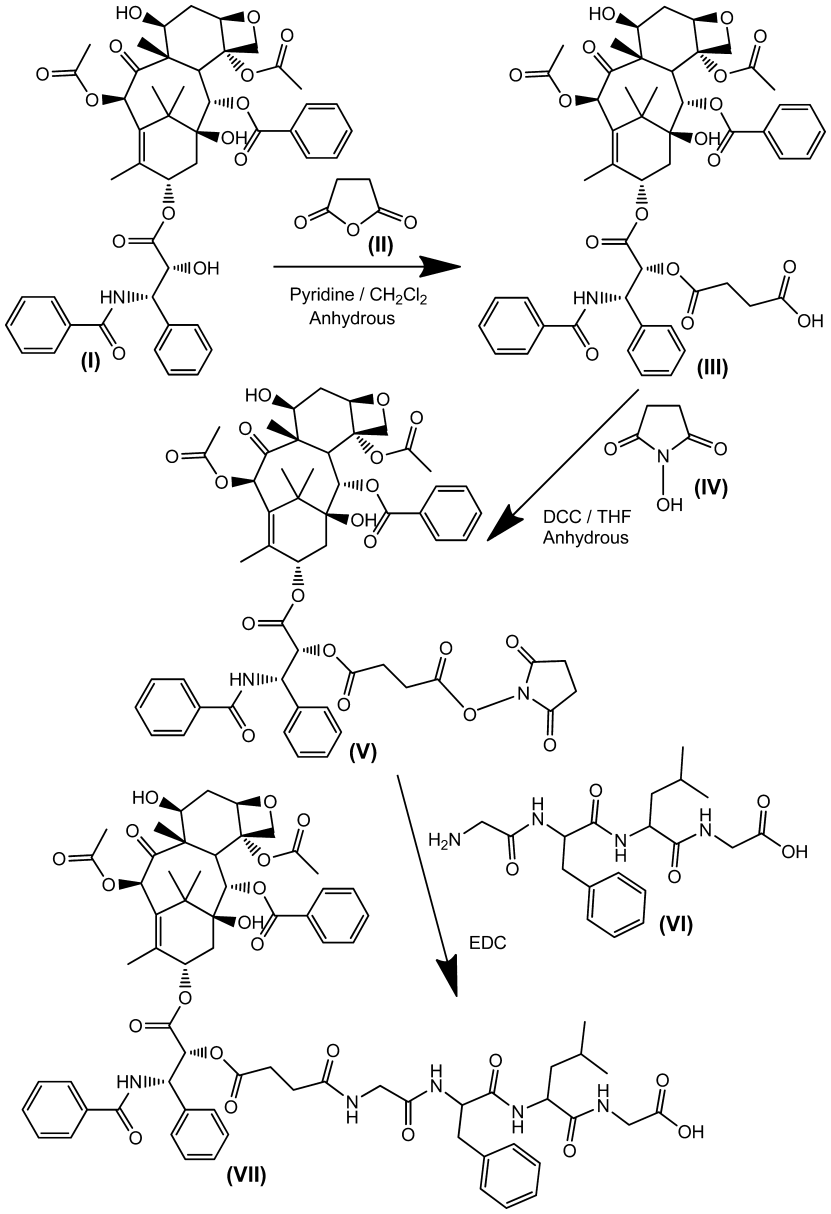

mg/mL.[8−10] To overcome this issue, PTX is currently administered as a 1.3% solution in Cremophor EL, a polyethoxylated castor oil excipient known to generate severe side effects such as bronchospasms, hypotension, hypersensitivity, nephrotoxicity, and neurotoxicity.[6,11−13] Though pretreatment with corticosteroids and antihistaminics takes care of majority of symptoms of hypersensitivity, 5−30% of patients treated with the Cremophor EL formulation of PTX still develop hypersensitivity and related problems.[14]

In recent years, innovative approaches have been investigated using alternative drug carriers or pro-drug designs to enhance drug bioavailability at the site of needed action;[15] however, many of these devices fail the "reality checks" of biological systems, such as phagocytic clearance in the vascular system and rejection by membrane transporters. In this context, an attractive strategy is the synthesis of a stable derivative that may possess better solubility in polar conditions and may release the active ingredient at the site of action. Some solubility-moderating polymeric conjugates of PTX have been designed, and clinically useful outcomes are awaited, but the approach is considered promising.[16] Solubility of dendrimers, a class of repetitively branched monodisperse polymers, can be tailored by the manipulation of their terminal functional groups, and therefore, they are very versatile and promising for the modulation of solubility of a drug. Dendrimers, terminally derivatized with hydrophilics (such as hydroxyl, amino, and carboxyl groups), are water-soluble.[17] Polyamidoamine (PAMAM) dendrimer is terminated by primary amino group and is commonly used for enhancing availability of carried drug in aqueous conditions. They are smart macromolecules, and the change in their conformations relative to their molecular weight and size (1 nm per generation), terminal functional groups, and external environment can be exploited for the purpose of an efficient drug delivery.[18] Their actions can be affected and manipulated by the biochemical environment defined commonly by the polarity, pH, and ionic conditions of the biological fluids around.[19] Also, generation-4 (G4) PAMAM dendrimers have been reported to demonstrate bioperme-

dx.doi.org/10.1021/mp500128k | *Mol. Pharmaceutics* 2014, 11, 1906−1918

Scheme 2. Synthesis of Paclitaxel−GFLG−Dendrimer (PGD or IX) Conjugate from Paclitaxel−GFLG Precursor and PAMAM Dendrimer

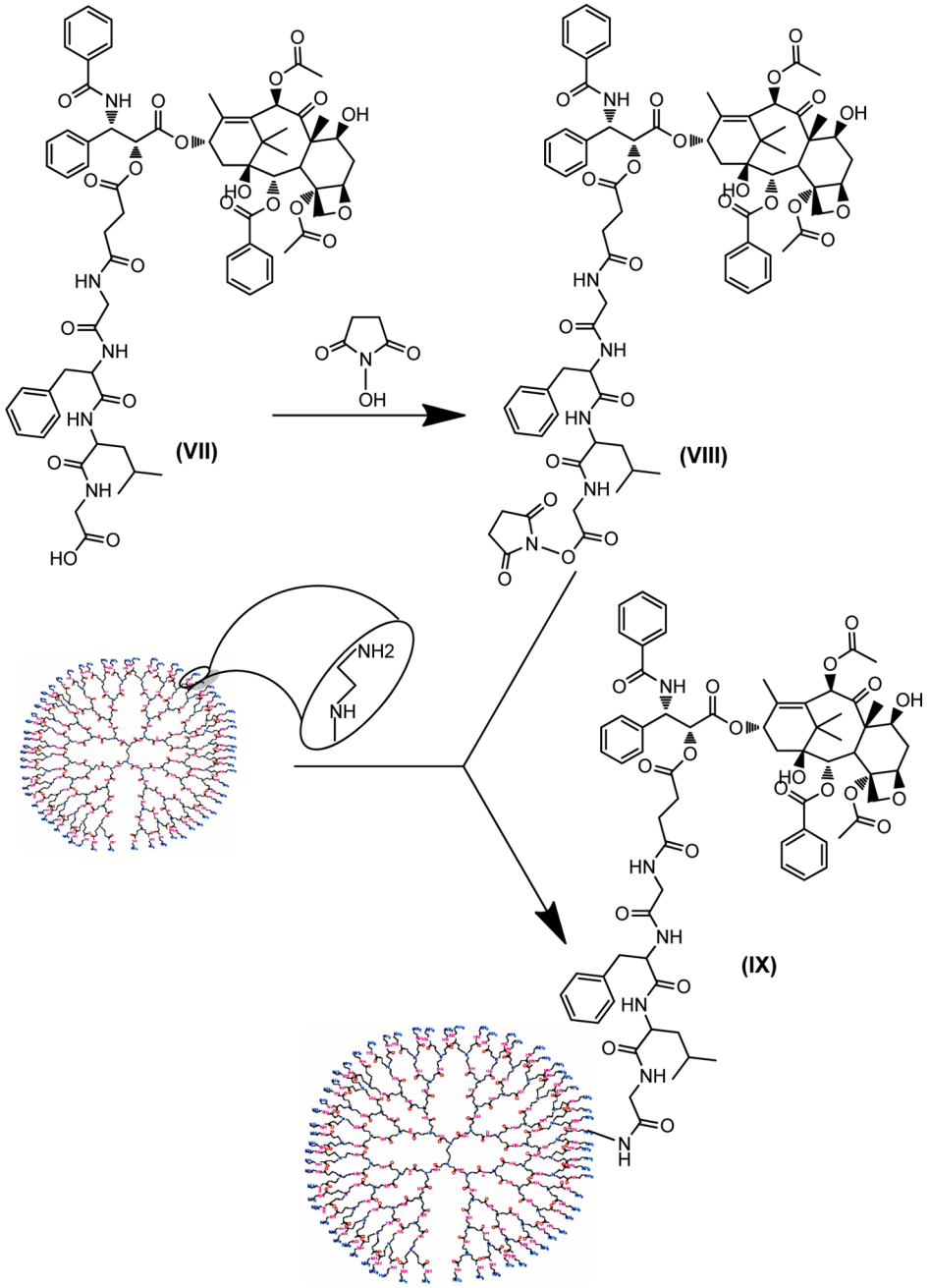

ability.[20] These factors allow PAMAM dendrimers to be an effective vehicle to enhance the availability and delivery of drugs, particularly PTX, in biological conditions.[21]

The other major problem encountered during PTX chemotherapy is its significant toxicity due to the nonspecific and indiscriminate distribution of the drug among the tissues. The primary mechanism of action of PTX is its induction of apoptosis by binding to microtubules within a dividing cell during mitosis, causing kinetic stabilization and inhibition of microtubule depolymerization that leads to mitotic arrest and the blockage of cell cycle progression.[22−24] This mechanism is nonspecific and results in serious unwanted consequences. One way to possibly enhance availability of PTX in biofluids and to introduce specificity at the same time is to couple PTX to PAMAM dendrimer using a bioactive linker, which targets a biomolecule that is overexpressed in the cancerous tissue in question. Such a strategy of "active targeting" helps at least in greatly reducing undesirable side effects to the rest of the body.[24−27]

Cathepsin B, a lysosomal enzyme, is up-regulated in breast cancer cells[28,29] and in highly metastatic breast tumors[30,31] compared to most other "normal" tissues. Barring exceptional conditions, cathepsin B is not found extracellularly in normal tissue; therefore, pro-drugs that target cathepsin B should remain stable in circulation[32] and should refrain from exhibiting toxic affects before they are hydrolyzed by cathepsin B. Consequently, in this work cathepsin B was targeted as a cellular enzyme that would cleave the drug attached to the PAMAM dendrimer, given that the linker between them is its substrate. One such substrate is a tetrapeptide, glycine-

dx.doi.org/10.1021/mp500128k | Mol. Pharmaceutics 2014, 11, 1906−1918

phenylananine-leucine-glycine (GFLG) that is cleaved by cathepsin B and allows liberation of the attached active ligand after endocytosis.[33,34] Polymers with intense three-dimensional (3D) molecular structure (such as dendrimers) make enzymatic release sterically challenging compared to linear polymers such as poly(ethylene glycol) (PEG) and *N*-(2-hydroxypropyl) methacrylamide (HPMA). Therefore, use of linkers that provide spacing from the dendrimer surface for easy access to the reactive site on drug molecules and specificity for enzymatic cleavage is essential. GFLG has been used as such a cleavable linker for cathepsin B induced drug delivery,[34,36] including the cancer therapy.[35,37]

On the basis of the above information, it was logical to explore if the conjugation of PTX to a PAMAM dendrimer through a cathepsin B cleavable linker would result in the synthesis of an active-targeting pro-drug version of PTX to demonstrate an improvement in its *in vitro* efficacy on breast cancer cells that have higher levels of enzyme and *in vivo* efficacy on xenograft tumors. Therefore, this study reports the synthesis of a pro-drug conjugate of PTX to a generation-4 PAMAM dendrimer via ester, amide, and peptide linkages, incorporating a GFLG linker. The conjugate and the intermediates prepared to reach to the product were characterized using physicochemical techniques as needed. The prodrug, paclitaxel−GFLG−dendrimer (PGD or IX) thus synthesized was evaluated for its *in vitro* activities against breast cancer cells and normal kidney cells, relative to those of PTX. Confirmation of increased toxicity by PGD against breast tumors in 3D, physiological conditions was performed using xenograft mice models.

EXPERIMENTAL SECTION

Syntheses. Starting from PTX, the synthesis of PGD was accomplished via five steps, the diagrammatic representation of which is portrayed in Schemes 1 and 2. While Scheme 1 displays the synthesis of the paclitaxel−GFLG conjugate, its further conjugation to PAMAM dendrimer is illustrated in Scheme 2.

Paclitaxel Hemisuccinate (III, Scheme 1). Compound III was prepared using the method of Majoras et al.[38] Briefly, PTX (I, Scheme 1; ChemieTek, Indianapolis, IN) was reacted with an excess of succinic anhydride (II, Scheme 1; Aldrich, Milwaukee, WI) in anhydrous methylene chloride in the presence of a catalytic amount of anhydrous pyridine. After the reaction was confirmed to be complete by thin layer chromatographic (TLC) analysis, pyridine was neutralized with dilute aqueous solution of hydrochloric acid and extracted. The residue, recovered from the organic phase after solvent evaporation, was recrystallized with acetone/water to get needle like crystals of III in almost quantitative yield; mp 177−179 °C;[39] TLC R_f (silica gel-G/hexane−ethyl acetate (all from Aldrich, Milwaukee, WI); 20:80) 0.17; HPLC (5 μL of 1 mg/mL sample was eluted isocratically with a mixture of water/acetonitrile; 55:45 at 1.5 mL/min through a C-18 modified silica particles of 5 μm size packed in a 3.9 × 300 mm Waters μ-Bondapak HPLC column; monitored spectrophotometrically at 215 nm; chart speed 1 cm/min) RT = 6.0 min.

^{1}H NMR [in $CDCl_3$ (Aldrich); referenced to δ 0.00 ppm for tetramethyl-silane (TMS; Aldrich) used as internal standard (IS)]: δ (ppm) 1.15 and 1.25 (s, 3H + 3H, 16-CH3 and 17-CH3), 1.7 (s, 3H, 19-CH3), 1.9 (s, 3H, 18-CH3), 2.20 (dd, 2H, 6-CH2), 2.25 (s, 3H, 29-CH3), 2.40 (dd, 2H, 14-CH2), 2.45 (s, 3H, 31-CH3), 2.6 and 2.75 (m, 2H + 2H, X-CH2 and X′-CH2), 3.8 (d, 1H, 3-CH), 4.20 and 4.33 (d + d, 2H, 20-CH2), 4.45 (dd, 1H, 7-CH), 4.97 (d, 1H, 5-CH), 5.5 (d, 1H, 2-CH), 5.7 (d, 1H, 2′-CH), 6.0 (dd, 1H, 3′-CH), 6.25 (t, 1H, 13-CH), 6.3 (s, 1H, 10-CH), 7.18 (d, 1H, N−H), 7.35 (m, 5H, 3′-C_6H5), 7.45−7.8 (m, 5H + 5H, 4′-C_6H5 + 21-C_6H5).

Paclitaxel Hemisuccinate, *N*-Hydroxysuccinimide Ester (V, Scheme 1). Compound V was synthesized by the method of Ryppa et al.[40] Briefly, an equivalent mixture of III, *N*-hydroxy-succinimide (IV, Scheme 1; Aldrich; 92 mg; 800 μM), and *N*,*N*-dicyclohexyl-carbodiimide (DCC; Aldrich) were reacted in anhydrous tetrahydrofuran (Aldrich) overnight. The mixture was precipitated with diethyl ether (Aldrich) and filtered. The organic filtrate was rotary-evaporated to get a residue, which was purified chromatographically on silica gel using a mixture of hexane/ethyl acetate (1:2) as eluent. After removal of solvent from the eluate, the product was obtained as white residue (93% yield) with following properties: TLC R_f (silica gel-G/hexane−ethyl acetate; 20:80) 0.80.

^{1}H NMR (in $CDCl_3$; referenced to δ 0.00 ppm for TMS, used as IS): δ (ppm) 1.15 and 1.25 (s, 3H + 3H, 16-CH3 and 17-CH3), 1.7 (s, 3H, 19-CH3), 1.95 (s, 3H, 18-CH3), 2.15 (dd, 2H, 6-CH2), 2.25 (s, 3H, 29-CH3), 2.35 (d, 2H, 14-CH2), 2.45 (s, 3H, 31-CH3), 2.5−2.65 (complex m, 2H + 2H, X-CH2 and X′-CH2), 2.85−2.95 (complex m, 2H + 2H, N−CH2 and N′-CH2), 3.82 (d, 1H, 3-CH), 4.20 and 4.35 (d + d, 2H, 20-CH2), 4.45 (distorted t, 1H, 7-CH), 4.97 (dd, 1H, 5-CH), 5.5 (d, 1H, 2-CH), 5.74 (d, 1H, 2′-CH), 6.0 (dd, 1H, 3′-CH), 6.25 (t, 1H, 13-CH), 6.3 (s, 1H, 10-CH), 7.18 (d, 1H, N−H), 7.35 (m, 5H, 3′-C_6H5), 7.45−7.75 (m, 5H + 5H, 4′-C_6H5 + 21-C_6H5).

Paclitaxel−Hemisuccinamide Derivative of GFLG (VII, Scheme 1). A mixture of III (Scheme 1, 764 mg; 800 μM), IV (92 mg; 800 μM), and 1-ethyl, 3-(3-dimethylamino-propyl)-carbodiimide hydrochloride (EDC-HCl; Aldrich; 153.6 mg; 800 μM) in an organic solvent was stirred overnight to form V (Scheme 1). The reaction was proceeded in to the next step without isolation and purification of V. GFLG tetrapeptide (VI, Scheme 1; Biomatik Corp., Wilmington, DE; 305.6 mg; 800 μM) and *N*-methyl-morpholine (NMM; Aldrich; 60 μL) were then introduced into the flask, and the reaction mixture was further stirred at room temperature overnight. The product was chromatographed on silica. After solvent removal and drying the residue under vacuum, 915 mg (86% yield) of VII was obtained with the following properties: TLC R_f (silica gel-G/EtOAc/methanol; 90:10) 0.29; HPLC (chromatographic conditions same as for III) RT = 2.5 min.

^{1}H NMR (in DMSO-d_6; referenced to δ 0.00 ppm for TMS as IS): δ (ppm) 0.82 and 0.87 [d + d, 3H + 3H, Leu-ω(CH3)2], 1.0 and 1.05 (s + s, 3H + 3H, 16-CH3 and 17-CH3), 1.5 (s, 3H, 19-CH3), 1.55−1.7 (complex m, 5H, 6-CH2, Leu-γCH, Leu-CH2), 1.8 (s, 3H, 18-CH3), 2.1 (s, 3H, 29-CH3), 2.25 (s, 3H, 31-CH3), 2.42 (d, 2H, 14-CH2), 2.8 (dd, 2H, X-CH2), 3.0 (dd, 2H, X′-CH2), 3.60 (complex, 2H, phenylalanine-CH2), 3.75 (complex, 1H, 3-CH), 4.0 [s, 4H, 2 X Gly-CH2)], 4.1 and 4.3 (d + d, 2H, 20-CH2), 4.5−4.6 (complex, 1H + 1H, 7-CH + Leu-αCH), 4.92 (distorted t, 1H + 1H, 5-CH + phenylalanine-α-CH), 5.3 (d, 1H, 2-CH), 5.4 (d, 1H, 2′-CH), 5.8 (complex m, 1H + 1H, 3′-CH + 13-CH), 6.3 (s, 1H, 10-CH), 7.16−8.16 (multiple m, 20H, aromatic-H + 5-amidic N−H).

***N*-Hydroxysuccinimide Ester of Paclitaxel−Hemisuccinamide Derivative of GFLG (VIII, Scheme 2) and Coupling of PTX to G4- PAMAM Dendrimer, Using**

GFLG as Linker (Collectively in One Unit Referred As Paclitaxel−GFLG−Dendrimer; Abbreviated as PGD or IX, Scheme 2). Compound VII (Scheme 2, 800 mg; 600 μM), NHS (69 mg; 600 μM) and EDC-HCl (115 mg; 600 μM) were reacted by stirring for 8 h at room temperature to form the *N*-hydroxysuccinimide ester of paclitaxel−hemisuccinamide derivative of GFLG (VIII, Scheme 2). The reaction was forwarded to the next step without isolating and purifying VIII. Then, G4-PAMAM dendrimer (Aldrich; 1.075 g; 75 μM) was introduced to the above reaction mixture containing VIII. The resultant mixture was again stirred at room temperature for overnight. The product was dissolved in a mixture of acetonitrile/water (2:1; 20 mL) and dialyzed against a mixture of acetonitrile/water (2:1). After evaporation of acetonitrile, the purified sample in residual water was lyophilized and then dried under vacuum to get IX (Scheme 2) in 75% recovery, with the following analytical characteristics.

Analyses. (i) HPLC [chromatographed isocratically on a 3.9 mm × 300 mm, Waters μ-Bondapak column packed with 5 μm size, C18-derivatized silica particles, eluted with H_2O/acetonitrile (55:45; 1.5 mL/min) at a pressure of 3000 psi. The eluted components were monitored spectrophotometrically at 215 nm: RT 8.7 min. (chart speed: 1 cm/min).

(ii) ^{1}H NMR (in DMSO-d_6: referenced to δ 0.00 ppm for TMS as IS): δ (ppm) 0.80 and 0.85 [d + d, 3H + 3H, Leu-ω(CH3)2], 1.0 (s + s, 6H, 16-CH3 and 17-CH3), 1.5 (s, 3H, 19-CH3), 1.55−1.7 (complex m, 5H, 6-CH2, Leu-γCH, Leu-CH2), 1.8 (s, 3H, 18-CH3), 2.0 (s, xH, from dendrimer), 2.1 (s, 3H, 29-CH3), 2.24 (s, 3H, 31-CH3), 2.42 (d, 2H, 14-CH2), 2.7 (broad, xH, from dendrimer), 2.8 (dd, 2H, X-CH2), 2.9 (dd, 2H, X′-CH2), 3.1 (broad, xH, from dendrimer), 3.60−3.75 (complex m, 2H + 1H, phenylalanine-CH2 and 3-CH, respectively), 3.9−4.05 [complex, 2H + 2H, 2 X Gly-CH2)], 4.1 and 4.25 (complexes, 2H, 20-CH2), 4.5 (m, 1H, Leu-αCH), 4.6 (t, 1H, 7-CH), 4.85−4.95 (complex m, 1H + 1H, 5-CH + phenylalanine-α-CH), 5.4 (complex m, 1H + 1H, 2-CH and 2′-CH), 5.87 (t, 1H, 13-CH), 6.15 (d, 1H, 3′-CH), 6.3 (s, 1H, 10-CH), 7.06−8.4 (multiple m, amidic N-Hs + aromatic-Hs).

(iii) Estimation of a number of PTX units per molecule of PGD: The quantitation of ligation of the paclitaxel−hemisuccinimide derivative of GFLG (VII) units per dendrimer molecule in PGD was done by NMR analysis using fumaric acid as IS. Thus, a mixture of PGD (5.5 mg; 0.228 μmol) and fumaric acid (Aldrich; 2.675 μg; 2.305 μmol) was taken in 600 μL of DMSO-d_6 (Aldrich) and the ^{1}H NMR spectrum was scanned. The spectrum exhibited all of the signals recorded for IX above, in addition to the one for methylene protons [−(**H**)C═C(**H**)−] of fumaric acid. The comparison of proton integration of the chemical shift signal at δ6.3 (10-C**H** of PTX moiety) relative to that of the chemical shift signal at δ6.6 [−(**H**)C═C(**H**)− of fumaric acid] yielded the quantitation of PTX moieties in the used amount of PGD, from which the molecular units of VII per dendrimer molecule was established.

(iv) MALDI-TOF mass spectrometry analysis of PGD was performed to support molecular weight determination using NMR method at the University of Texas Health Science Center at San Antonio (UTHSCSA) Department of Molecular Medicine Mass Spectrometry core service.

Confirmation of Activity of a Cathepsin Homologue on PGD. Enzymatic activity of papain, a homologue of cathepsin B[41,42] against the PGD was verified for hydrolytic release of paclitaxel−GFLG from the conjugate. PGD conjugate (1 mg/mL, n = 3) was reacted at 37 °C in reaction buffer (0.1 M acetate, 0.01 M EDTA, and 0.05 M reduced glutathione)/organic solvent mixture in the presence or absence (control) of 0.5×10^{-6} M papain. Samples were analyzed by HPLC after 24 h. Aliquots of both control and enzyme-digested samples were analyzed at the Texas A&M University Laboratory for Biological Mass Spectrometry (TAMU-LBMS; College Station, TX) by the liquid chromatography−mass spectrometry (LC−MS) analysis.

Cell Cultures. MDA-MB-231, MDA-MB-468, BT-20, and T47-D human breast cancer cells along with mouse proximal tubule kidney cells BUMPT were cultured in RPMI 1640 medium (Life Technologies, Carlsbad, CA). MDA-MB-435 human breast cancer cells and JEG-3 human choriocarcinoma cells were maintained in DMEM (Life Technologies). Both media were supplemented with 10% heat-inactivated FBS (Hyclone Laboratories, Logan, UT), 1% Glutamax (Life Technologies), and penicillin (100 IU/mL)/streptomycin (100 μg/mL)/amphotericin B (0.25 μg/mL) (Life Technologies, 15240-062). All cell lines were maintained at 37 °C in a humidified incubator in a 5% carbon dioxide atmosphere.

Western Blot Analysis. Cellular lysates for Western blot analysis were prepared using previously described methodology.[43] Briefly, cells were washed three times with phosphate-buffered saline (PBS), treated with cold RIPA lysis buffer [50 mM Tris-HCl, 150 mM NaCl, 0.5% Nonidet P-40, 0.1 sodium dodecyl sulfate (SDS), 0.1% sodium deoxycholate, 1× protease inhibitor mixture (Roche Biochemical), and 1 mM sodium vanadate] on ice for 20 min, and harvested by scraping. Lysates were centrifuged at 14,000*g* for 15 min at 4 °C and supernatant was collected. Protein concentrations were determined using microbicinchoninic acid (BCA) assay (Thermo Fisher Scientific, Rockford, IL) and proteins were stored at −80 °C. Cell lysates containing equal amounts of protein (~20 μg) were electrophoresed on 8% SDS-polyacrylamide gels and transferred onto a 0.2 μm nitrocellulose membranes. Blots were probed with appropriate antibodies. Actin and cathepsin B proteins were probed using antiactin antibody produced in rabbit (Sigma-Aldrich, St. Louis, MO) and anticathepsin B monoclonal mouse antibody (Sigma-Aldrich), respectively, as primary antibodies. After staining with appropriate secondary antibodies, blots were developed using enhanced chemiluminescence method.

Metabolic Activity Assay. The effect of PGD on metabolic activity was determined by 4-[3-(4-iodophenyl)-2-(4-nitrophenyl)-2*H*-5-tetrazolio]-1,3-benzene disulfonate (WST-1) assay (Roche Diagnostics, Indianapolis, IN). Cells (2×10^3 cells/well) were seeded in 96-well culture plates and incubated for 24 h. Previous media was aspirated and replenished with fresh RPMI 1640 culture medium supplemented with 5% FBS, 1% Glutamax, and penicillin (100 IU/mL)/streptomycin (100 μg/mL)/amphotericin B (0.25 μg/mL) (Life Technologies, 15240-062) and containing PTX or PTX-equivalent PGD. To determine optimal treatment concentrations to observe drug effects, MDA-MB-231 cells were first treated with various concentrations of PTX or PTX-equivalent PGD (0.01 nM to 1 μM). Subsequent analysis on a panel of cancer cells and normal kidney cells were performed at 5 and 10 nM PTX or PTX-equivalent PGD, approximately two to three times the IC_{50} concentration for PTX against MDA-MB-231 cells. Media alone served as a blank, and plain, unloaded PAMAM at equimolar concentration was the negative control. After 72 h, 10 μL of WST-1 reagent was added to each well and plates were incubated for an additional 4 h.

Absorbance of the converted WST-1 product was read at 415 nm on a microplate reader (Biotek Synergy 2). The relative IC_{50} data were calculated by GraphPad Prism 5 (GraphPad Software, La Jolla, CA).

Apoptosis Assay. Annexin staining for measurement of apoptosis was performed with the use of a kit (FITC Annexin V Apoptosis Detection Kit II; BD Pharmingen, San Jose, CA). Briefly, MDA-MB-231 cells were seeded at 10^6 cells/dish and incubated for 24 h. The cells were then treated with 50 nM PTX or PTX-equivalent PGD. Media alone served as blank. After 48 h of treatment, cells were washed with cold PBS and resuspended in 100 μL binding buffer. Cells were stained with 5 μL of FITC Annexin V and 5 μL of propidium iodide (PI) for 15 min in the dark before diluting with an additional 400 μL binding buffer. Samples were analyzed by flow cytometry on a FACS Calibur (BD Biosciences, San Diego, CA).

***In Vivo* Antitumor Efficacy.** All animal experiments were performed after obtaining approval from the UTHSCSA Institutional Animal Care and Use Committee, and animals were housed in accordance with the UTHSCSA institutional protocol for animal experiments.

MDA-MB-231 cells were resuspended in 50% v/v serum-free culture medium/Matrigel Matrix (BD Biosciences, San Jose, CA). Approximately 2×10^6 MDA-MB-231 cells (100 μL) were injected into the mammary fatpad of 6 to 7-week-old female athymic nude mice. Once tumor masses in xenografts reached an average volume of 90 mm^3 (about 8 days after innoculation), mice were randomly assigned to four groups (n = 7): control (saline vehicle), PTX (10 mg/kg), PGD (40 mg/kg or PTX-equivalent), and unloaded PAMAM dendrimer (negative control; 24 mg/kg or PGD-equivalent). Mice were given injections every other day intraperitoneally for a total of 3 injections. Two-dimensional tumor measurements were made weekly after the first dose. The tumor volume was calculated according to the following formula:

$$\text{volume} = (\text{short diameter}^2) \times (\text{long diameter}) \times 0.5$$

The extent of tumor burden per animal was expressed in cubic millimeters. Mice were sacrificed 24 days after treatment initiation.

Statistical Analysis. Data are presented as the mean ± standard deviation (SD). One-way analysis of variance tests were used to investigate the differences between groups for apoptosis in vitro experiments and two-way analysis of variance tests for *in vivo* and metabolic activity *in vitro* experiments, followed by *post hoc* tests with Bonferroni correction for comparison between individual groups. Statistical significance was established at $p < 0.05$. Data for metabolic activity assays was investigated using Stata/IC 12.0 (StataCorp LP, College Station, TX). All other experiments were analyzed using GraphPad Prism 5 (GraphPad Software, La Jolla, CA).

RESULTS AND DISCUSSION

The goal of this work was to design a PTX-bound PAMAM dendrimer, using a cathepsin B-cleavable spacer for active-targeted delivery of PTX, and to examine the designed device for its enzymatic release, cellular toxicity/apoptotic activity, and capability to reduce tumor growth, compared to the activity of PTX alone. The design of cathepsin B targeting GFLG linked PTX–PAMAM conjugate was accomplished through a multi-step chemical synthesis as presented in Schemes 1 and 2.

For the conjugation of a drug molecule (i.e., PTX, here) to a supporting carrier molecule (i.e., PAMAM dendrimer, here), an important factor is the protection of reactive site(s) of drug molecule and retention of natural steric factors around it. Since, the direct attachment of drug molecule to carrier molecule may introduce crowding (steric effects) on the reactive sites of drug, invariably the drug molecules are attached to support molecule via a spacer arm that keeps a sufficient distance between the two to exclude the possibility of chemical damage to the reactive sites and the introduction of steric factors in drug molecule.[44,45] To retain bioactivity, it is essential to protect oxetane ring (covering C-4, C-5, and C-20), acetate group at C-4, benzoyl or related group at C-2, and benzamido and phenyl groups at C-3′ of PTX molecule (Figure 1).[46] However, the

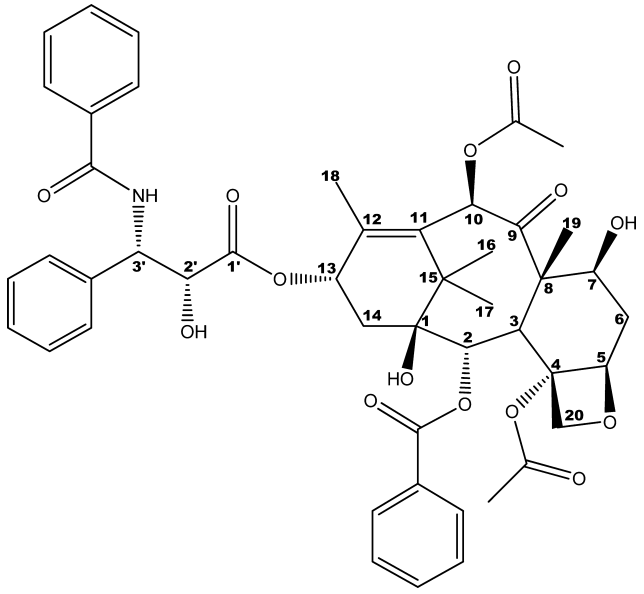

Figure 1. Chemical structure of paclitaxel.

molecule contains three hydroxyl groups that may be chemically modified for suitable structural manipulations. The hydroxyl group at C-1 has no considerable chemical activity; therefore, PTX prodrugs are generally designed by derivatizing the hydroxyl groups at C-2′ and/or C-7,[47] though the one at C-2′ is significantly more reactive than the one at C-7.[39] Hence, PTX was conjugated to PAMAM via a GFLG linker by derivatizing the hydroxyl group at C-2′ of the PTX. Thus, using a known methodology, PTX (I) was converted to its hemisuccinate (III) to acquire a terminal carboxy group on the molecule. The newly acquired carboxy terminus at position C-2′ of PTX was activated as *N*-hydroxysuccinimide (NHS) ester (V) and was reacted to amino terminus of GFLG tetrapeptide (VI). The carboxy-terminus of the resultant paclitaxel–hemisuccinate derivative of GFLG (VII) was again activated as NHS ester (VIII) to finally react to the amino groups of PAMAM (G4) dendrimer to get the required PTX conjugated dendrimer (IX or PGD) coupled by cathepsin B cleavable GFLG.

The identity of III was confirmed by its melting point being in agreement with that of the reported one[39] and by the presence of the triplets at δ2.6 and δ2.75 ppm in addition to the required peaks for PTX in its ^{1}H NMR spectrum, confirming the hemisuccinate derivatization of the OH group at C-2′ of PTX. Also, the proton at C-2′ showed up at δ5.53 ppm instead

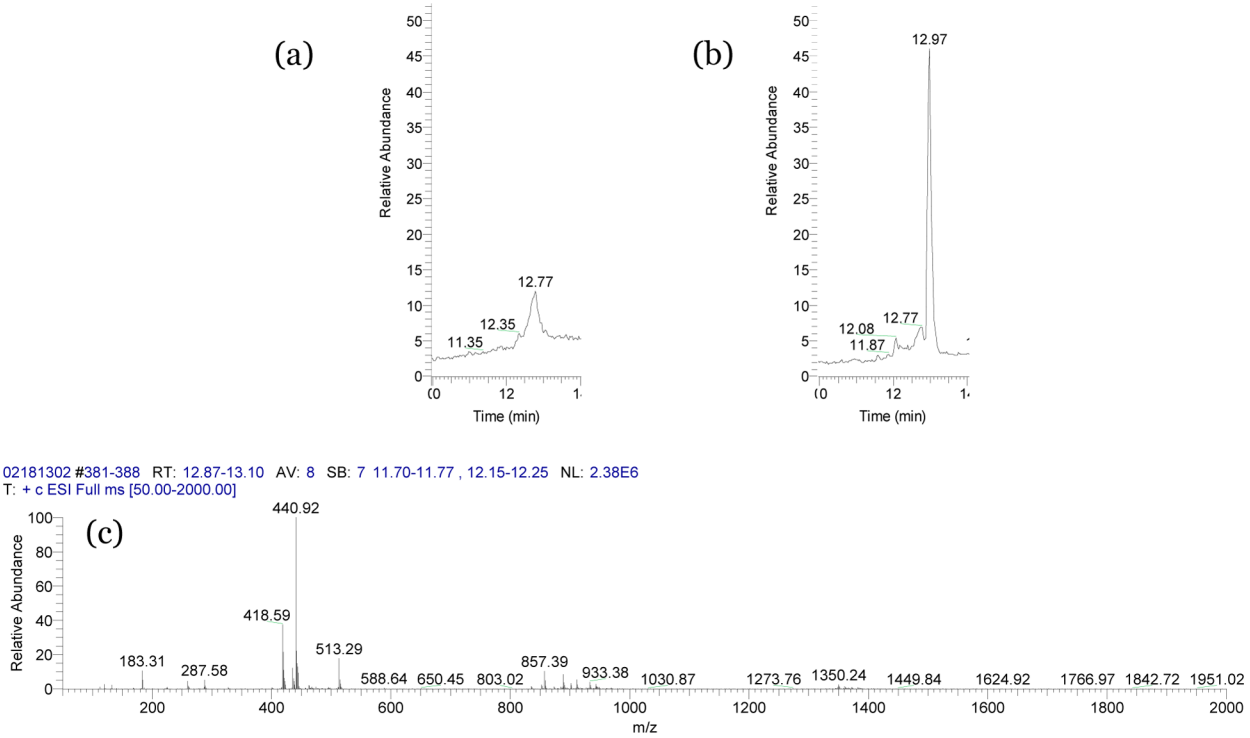

Figure 2. LC−MS analysis of PGD conjugates treated without and with papain, a cathepsin B-like enzyme. LC chromatograms of samples (a) without and (b) with papain are shown. A peak unique to papain-digested PGD sample was observed at 12.97 min, and (c) mass spectrometry results show a molecular ion peak at 1350 indicative of paclitaxel−GFLG (VIII).

of the proton geminal to "unsuccinated" OH at the same position in PTX at δ4.80 ppm. The formation of V was clearly indicated by the chromatographic separation of V from III when cospotted in a chromatogram over SiO_2-G and developed by hexane/ethyl acetate; 20:80 (R_fs: 0.17 and 0.80 for III and V, respectively). The structural conformation of V was done by ^{1}H NMR as it recorded the presence of a complex multiplet at δ2.85−2.95 for the two methylene groups (N−CH2 and N′-CH2) of succinimide terminus, while keeping those for two hemisuccinate methylenes as in III. The formation of VII was similarly indicated by the chromatographic separation of VII from V when cospotted in chromatogram over SiO_2-G and developed by ethyl acetate/methanol; 90:10 (R_fs: 0.92 and 0.29 for V and VII, respectively). In the ^{1}H NMR spectral analysis of VII, the absence of signals at δ2.85−2.95 for the two methylene groups (N−CH2 and N′−CH2) of succinimide terminus found in V, and instead, the presence of signals for leucine (at δ 0.80, 0.87, 1.55−1.7), for phenylalnine (at δ 3.60, 4.92), for glycine (at δ 4.0), and those for amidic N−Hs confirms the replacement of NHS group in V with the GFLG tetra-peptide to form VII.

The formation of the final product (IX) was indicated by the difference of HPLC retention time for IX compared to that for VII when eluted on a C-18 RP column with H_2O/acetonitrile (55/45) at 1.5 mL/min; while the retention time for VII was 2.5 min, IX was retained for 8.7 min. The ^{1}H NMR spectrum of IX retained the signals for VII with the addition of the ones at δ2.0, 2.7, and 3.1 (all specific to PAMAM dendrimer) confirmed the conjugation of VII to PAMAM dendrimer to form IX. Markedly improved solubility in polar solvents (a key factor in determining bioavailability) by the PGD conjugate was a strong physicochemical differentiator from the PTX molecule.

The number of PTX moieties attached per dendrimer entity in the final product (IX or PGD) was determined by using fumaric acid as an IS in ^{1}H NMR scanning. NMR peaks at δ6.3 and δ6.6 were integrated and the resulting peak areas were normalized per single proton. The ratio of the peak area of a proton of fumaric acid (derived from the signal at δ6.6) relative to the peak area of one proton from PTX (derived from the signal at δ6.3) is equivalent to the ratio of moles of fumaric acid over moles of PTX present. Given this, the total content of PTX, and by extension paclitaxel−GFLG, in solution was determined to be 1.662 μmol. The mass of paclitaxel−GFLG was subtracted from the total mass PGD introduced, yielding an estimated mass of PAMAM dendrimer. The ratio of the moles of PTX to the moles of PAMAM dendrimer was 7.112, suggesting approximately 7 PTX moieties were loaded per dendrimer unit. The estimated molecular weight was approximately 23,385 Da, as also confirmed by MALDI-TOF mass spectrometry, which showed a broad peak centered around 23−24 kDa. This ratio was used to create dilutions of PGD to deliver specific molar amounts of PTX in further biological experiments.

The ability of PGD to release paclitaxel-GFLG in the presence of papain, a homologue of cathepsin B, was evaluated in a 24 h reaction. Isocratic HPLC analysis of the reaction mixture showed the development of a new product peak in the chromatogram at 2.5 min, relative to the control sample (absence of papain). In subsequent analysis by LC−MS, the above enzymatic reaction mixture and the related control reaction mixture (without papain) were injected separately on a reverse phase C18, 150 × 2.1 mm column, and the chromatograms were developed for elution with the following gradient system at 0.3 mL/min: from 0−5 min, the eluent was 5% acetonitrile in 1% aqueous acetic acid solution, then a

gradient was run to bring the eluent composition to 100% acetonitrile by 20 min. The chromatogram for the PGD reaction with papain showed a peak at 12.97 min; this peak was absent in the reaction without papain (control sample) (Figure 2). Electrospray ionization (ESI) mass spectrum analysis of the content in the LC peak at 12.97 min revealed the molecular ion peak to be at 1350. This confirms the formation of VIII in papain degradation of PGD in a buffer solution that contains sodium ion. Molecules with multiple oxygens, including PTX, are known to form sodium adducts.[48,49] Therefore, the molecular ion peak for VIII shows the replacement of a proton in VIII with a sodium ion, i.e., $[M + Na]^+$ at m/e 1350. Thus, PGD was shown to release paclitaxel−GFLG (VIII) in the presence of cathepsin B-like enzyme.

To correlate the effect of PGD on metabolic activity with the presence of cathepsin B, the levels of total cellular cathepsin B were investigated in an array of cells by Western blot and enzymatic assays. Six breast cancer cell lines (MDA-MB-231, MDA-MB-468, MDA-MB-435, BT-20, BT-549, and T47D) that demonstrate PTX sensitivity were chosen to represent the diseased state. Breast cancer with choriocarcinomatous features represents a distinct subset of the breast cancer spectrum, with 12−33% of female breast cancer patients expressing human chorionic gonadotropin (hCG).[50,51] As such, the human choriocarcinoma cell line JEG-3 was chosen as a model to represent such pathological features. Finally, renal clearance is one of the primary methods of nanoparticle removal from the body. Given its large blood flow and ability to concentrate toxic compounds, the kidneys are also particularly sensitive to xenobiotics.[52] As such, BUMPT mouse kidney proximal tubule cells were chosen as a model for nanoparticle behavior against this critical normal tissue.

Cathepsin B was detected in all cells, an expected result given its presence in the lysosome of normal cells (Figure 3). However, marked differences were seen in its levels in the normal BUMPT mouse kidney proximal tubule cell line relative to that determined in the cancer cell lines. Western blot analysis showed that cathepsin B had the highest presence in T47D cells, followed by a medium level of presence in decreasing order in JEG-3, MDA-MB-435, MDA-MB-468, MDA-MB-231, and BT-20 cancer cells. Finally, the lowest presence was observed in the BT549 cancer cell and BUMPT normal mouse kidney proximal tubule cell line.

The effect of PGD on metabolic activity was studied. Metabolic activity assays, such as the WST-1 assay, have been previously established as indirect methods of assessing cytotoxic activity of drugs.[53,54] To ascertain an optimal treatment concentration with which to study drug effects, MDA-MB-231 cells were first treated with various concentrations of PTX and PTX-equivalent PGD (Figure 4). The relative IC_{50} concentration is the halfway point between the top and bottom plateaus of the concentration curve.[55] When comparing the IC_{50} of PTX relative to PGD, a marked leftward shift was observed at 3.29 and 0.640 nM, respecitively. This suggested an increased cytotoxic profile for PGD as compared to PTX alone. A smaller concentration of PGD could deliver the same effect as a five times larger concentration of PTX, thereby increasing the efficiency of drug delivery. For further metabolic activity assays, PTX concentrations near 2× and 3× IC_{50} of PTX (5 and 10 nM) were used. This treatment range has been shown appropriate to evaluate drug therapies.[56−58]

A panel of 6 breast cancer cell lines, a choriocarcinoma cell line, and a normal kidney cell line were used as models to investigate the effect of PGD, and its unmodified predecessor PAMAM, on metabolic activity (Figure 5). The unconjugated

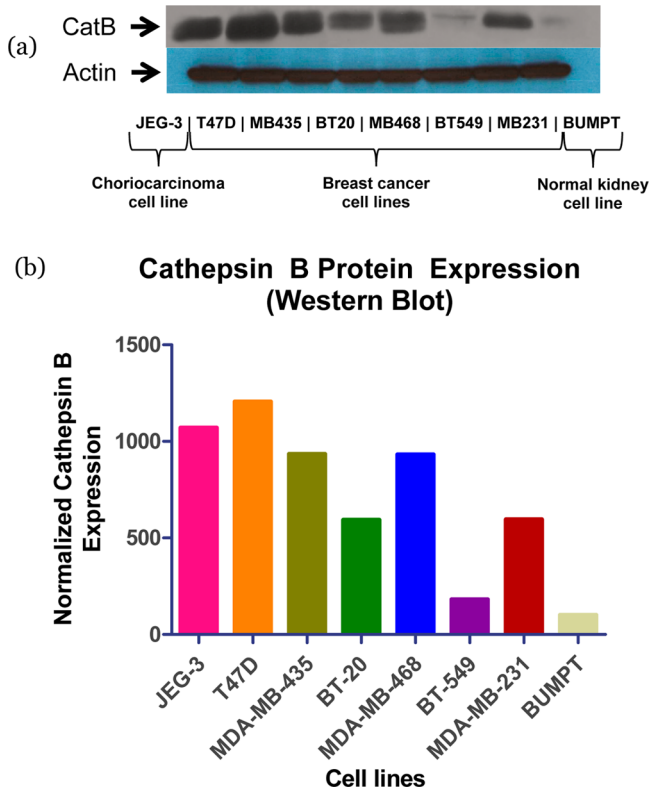

Figure 3. (A) Western blot analysis of cathepsin B in human breast cancer, human choriocarcinoma, and normal immortalized mouse kidney proximal tubule cells. Total cellular protein (20 μg) was electrophoresed on 8% SDS-PAGE gel and blotted onto a nitrocellulose membrane. Cathepsin B detection was performed by using anticathepsin B monoclonal mouse antibody, staining with horseradish peroxidase-conjugated secondary antibody, and developing with enhanced chemiluminescence method. (B) Densitometric analysis of cathepsin B Western blot was performed using Adobe Photoshop software (Adobe Systems, San Jose, CA), normalized to actin intensity, and expressed relative to BUMPT values.

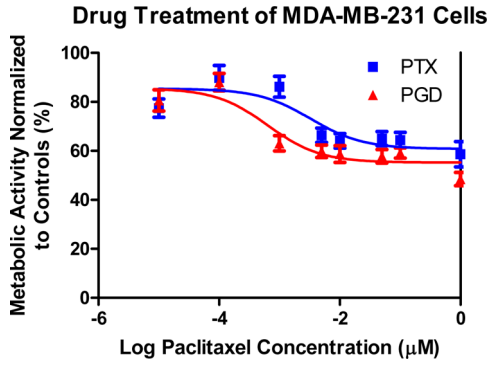

Figure 4. Effect of drug concentrations on MDA-MB-231 metabolic activity. Cells were exposed to PTX, PTX-equivalent PGD, and PGD-equivalent PAMAM at different concentrations (0.01 nM to 1 μM) for 72 h. 4-[3-(4-Iodophenyl)-2-(4-nitrophenyl)-2*H*-5-tetrazolio]-1,3-benzene disulfonate (WST-1) reagent was incubated for 4 h, and results are reported here as control-normalized means ± standard deviation of three independent experiments (n = 6). Nonlinear regression and relative IC_{50} data was calculated by GraphPad Prism 5 (GraphPad Software, La Jolla, CA).

dx.doi.org/10.1021/mp500128k | *Mol. Pharmaceutics* 2014, 11, 1906−1918

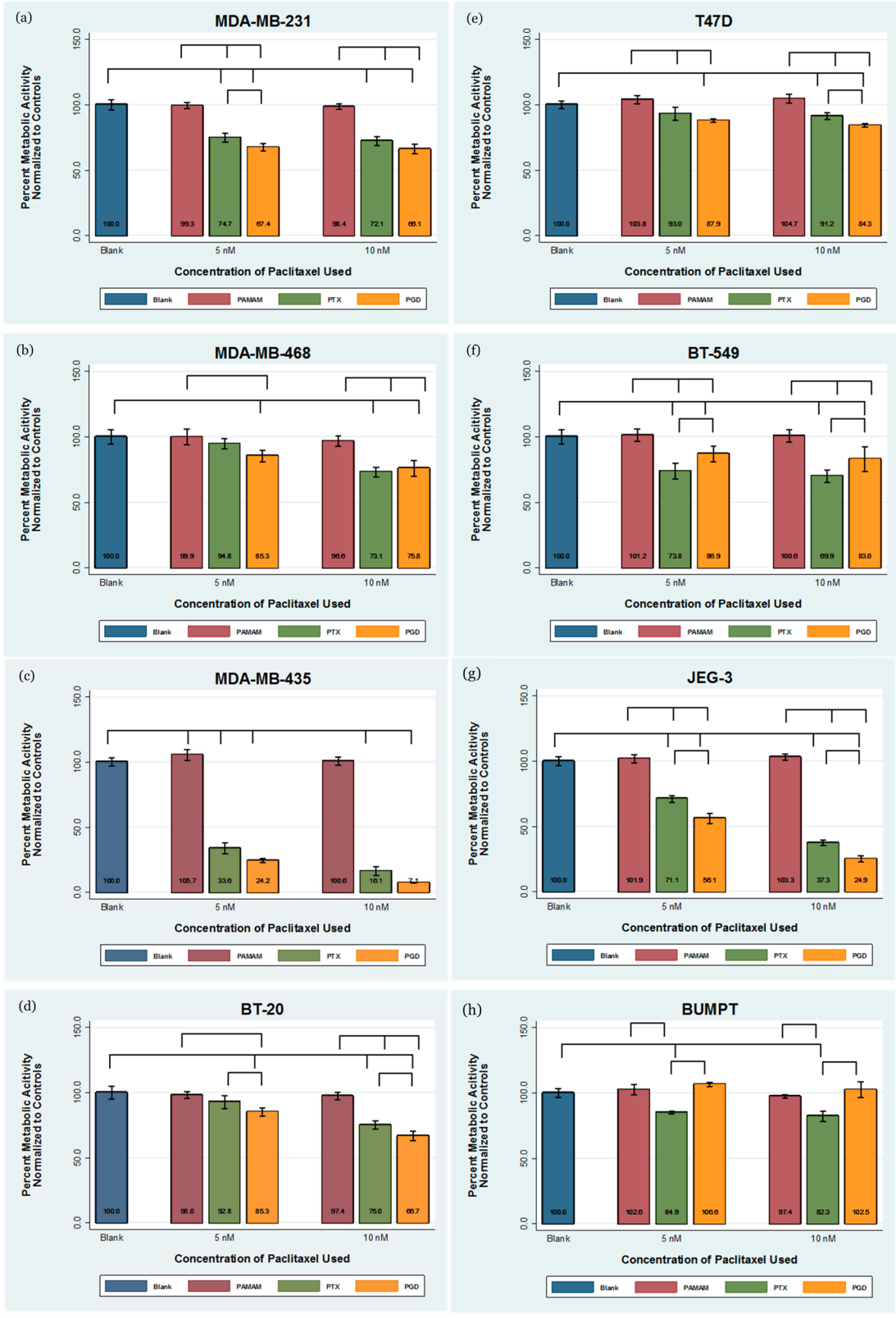

Figure 5. Effect of PGD on metabolic activity. 4-[3-(4-Iodophenyl)-2-(4-nitrophenyl)-2*H*-5-tetrazolio]-1,3-benzene disulfonate (WST-1) assay of (a) MDA-MB-231, (b) MDA-MB-468, (c) MDA-MB-435, (d) BT-20, (e) T47D, (f) BT-549, (g) JEG-3, and (h) BUMPT cells were treated with 5 and 10 nM PTX, PTX-equivalent PGD, or PGD-equivalent PAMAM for 72 h. MDA-MB-231, MDA-MB-468, MDA-MB-435, BT-20, T47D, and BT-549 are human breast cancer cell lines. JEG-3 is a human choriocarcinoma cell line. BUMPT is a mouse kidney proximal tubule cell line. Results are reported as mean ± standard deviation of three independent experiments ($n = 6$). Statistically significant results are indicated by grouped lines ($p < 0.05$).

dx.doi.org/10.1021/mp500128k | *Mol. Pharmaceutics* 2014, 11, 1906−1918

vehicle PAMAM served as a negative control. All cell lines demonstrated that there was no statistical difference between PAMAM treated (both 5 and 10 nM) samples and untreated samples. Cancer cell lines that had a moderate-to-high cathepsin B presence and enzymatic activity demonstrated stronger response to PGD treatment than PTX alone. JEG-3, MDA-MB-435, and BT-20 cell lines each had a statistically significant ($p < 0.05$) difference between the PGD and PTX response at both 5 and 10 nM concentrations. MDA-MB-231 and T47D cells demonstrated statistically significant differences between PGD and PTX response at only 5 and 10 nM concentrations, respectively, but not the other concentrations. MDA-MB-468 cells demonstrated no statistical significant metabolic activity response from PGD and PTX treatments at either 5 or 10 nM concentrations. However, only PGD treatment was statistically different from the untreated samples at the 5 nM concentration.

Cells with the lowest cathepsin B presence, the cancer cell line BT549 and the normal kidney cell line BUMPT, demonstrated an inverse of this relationship between PTX and PGD. The cytotoxic effect of PGD on metabolic activity was reduced in BT549 cells and eliminated in BUMPT cells. Treatment of cells with PTX still produced a statistically significant decrease in metabolic activity. Thus, from a broad perspective, cathepsin B levels correlate to PGD activity. Cells with a moderate-to-high cathepsin B activity showed a noticeable reduction in metabolic activity when treated with PGD as compared to PTX, while cells with low cathepsin B showed an inverse of this relationship. As cathepsin B is present at a very basal level under tight regulation in most normal tissues,[59,60] with expectedly similar expression profiles to that observed for BUMPT, these results suggest that PGD may lower toxicity from PTX treatment to normal tissues while maintaining or increasing therapeutic efficacy to cancer cells overexpressing cathepsin B. In particular, the results indicate potentially increased protection for the xenobiotic-sensitive kidneys.

This was verified by regression analysis between the magnitude of PGD-induced cytotoxic improvement at 10 nM treatment and cellular cathpesin B expression (Figure 6). PGD-induced mean metabolic activity was subtracted from PTX-induced mean metabolic activity for each cell line, resulting in a metabolic activity differential that was plotted against the cell line's cathepsin B expression. The coefficient of determination, r^2, was 0.652 at $p < 0.05$. This suggested a strong, statistically significant correlation between cathepsin B expression and increased ability of PGD to induce cytotoxicity compared to PTX (at 10 nM concentration).

Still, the correlation between cathepsin B expression and PGD-induced cytotoxicity is not a perfect positive fit, suggesting that factors other than cathepsin B expression alone may contribute to targeting effectiveness. In particular, recent work has suggested that PAMAM-based PTX conjugates adversely affect cell behavior by PTX-dependent and PTX-independent modes of action.[61] Similarly, beyond a threshold-level of total cellular cathepsin B activity, cell-dependent alternative mechanisms may be responsible for the variability in cell line response observed in our experiments, such as cell line-influenced nanoparticle absorption capability and replication rate. Alternatively, cell sensitivity to PTX may reflect on the ability of PGD dendrimer to elicit a larger response. Such mechanistic studies will be pursued in due course as they are beyond the scope of the current work.

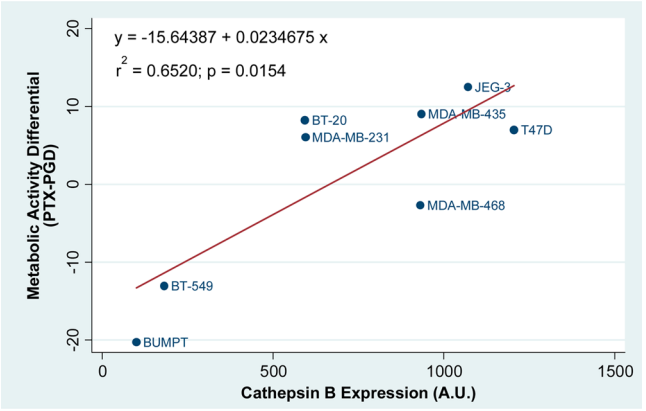

Figure 6. Regression analysis between magnitude of PGD-induced cytotoxic improvement (metabolic activity differential) at 10 nM treatment and normalized cathepsin B expression. At a 10 nM PTX-equivalent treatment, PGD-induced mean metabolic activity was subtracted from PTX-induced mean metabolic activity for each cell line, resulting in a metabolic activity differential. This was plotted against the respective cell line's cathepsin B expression as determined by densitometric analysis from Western blots.

MDA-MB-231 breast cancer cells were chosen as model cells for further studies due to their favorable response rates in the metabolic activity assays, appropriateness as models of malignant metastatic breast cancer phenotype, tumorigenicity *in vivo*, and well-characterized nature with regards to PTX response.[62,63]

To confirm if reduced metabolic activity by PGD conjugate was a result of cell death via the apoptotic pathway, annexin V-FITC staining was used to quantitatively determine the percentage of cells within a population that were undergoing apoptosis (Figure 7). MDA-MB-231 cells were treated for 48 h with 50 nM PTX, PTX-equivalent PGD, and PAMAM (as negative control). Our results indicate that PAMAM treatment produced no significant difference ($\alpha = 0.05$) in percent of cells stained with annexin V compared to untreated controls (28% versus 33%, respectively). By contrast, both PTX and PGD

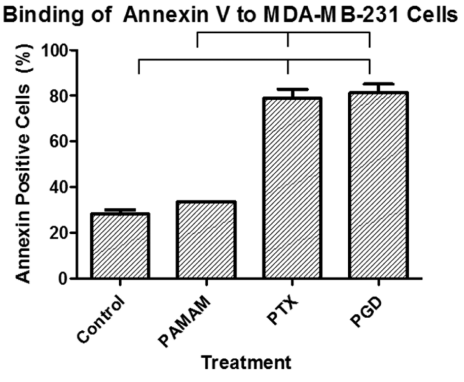

Figure 7. PGD exposure to MDA-MB-231 cells induces apoptosis. Annexin V staining was conducted with the use of a kit (Annexin V-FITC apoptosis detection kit; BD Pharmingen) and analyzed by flow cytometry. MDA-MB-231 breast cancer cells were exposed to 50 nM PTX, PTX-equivalent PGD, and PGD-equivalent PAMAM for 48 h. Untreated blank samples served as control. Results are reported as mean ± standard deviation of three independent experiments. Statistically significant results are indicated by grouped lines ($p < 0.05$).

treatments elicited a strong response with nearly 80% of cells analyzed staining positively for annexin V. Cells under PGD treatment had slightly stronger response with 81% of cells staining for annexin V as compared to 78% of cells under PTX treatment; these results were statistically differentiable from untreated cells (controls) but not from each other. The results suggested that cell death from the apoptotic pathway was a key component in the observed reduced proliferation rates in the WST-1 assays. Further, given the similarity in annexin staining, the underlying mechanisms responsible for apoptosis under PGD treatment were not altered from that of PTX treatment.

While our studies confirmed the cytotoxic behavior of PGD toward cancer cells during *in vitro* testing, two-dimensional cell cultures cannot replicate the cell−cell and cell−matrix interactions of the inherently three-dimensional system faced by drug delivery platforms *in vivo*, let alone the drastically different diffusion and transport properties.[64] The behavior of nanoparticles *in vivo* often differs significantly from the predicted behavior derived from *in vitro* cell culture studies.[65] As a result, to validate previous observations and discern new insights, the effect of PGD as compared to PTX on tumor growth was evaluated through *in vivo* xenograft studies using MDA-MB-231 cells. Mice treated from all groups survived until prescheduled termination of experiment 32 days after tumor inoculation. No treatment showed external toxic or lethal side-effects such as, furring, weakness, or fatigue.

Unloaded PAMAM dendrimer was tested as vehicle control to verify that it did not contribute to antitumor activity observed during PGD treatment. As can be seen (Figure 8), unloaded PAMAM was statistically indistinguishable at every measured time point from mice without treatment (saline injections). By contrast, treatment with PGD began to show reduced growth in tumor volume compared to control 1 week after treatment initiation and had statistically significant differences ($p < 0.05$) in tumor volume by weeks 2 and 3. PGD-treated tumor volumes were up to 58% and 49% smaller than controls for weeks 2 and 3, respectively. Mice treated with PTX had consistently smaller tumor volumes than control throughout the experiment as well. Yet, the tumor volumes were not significantly different ($p > 0.05$) from control until 3 weeks after treatment initiation, when PTX-treated tumor volumes were on average 23% smaller than controls. The growth of tumors treated with PGD was slower compared to those treated with PTX, resulting in statistically significant differences in tumor volume between the pair in weeks 2 and 3 after treatment initiation. PGD-treated tumor volumes were 48% and 34% smaller than PTX-treated tumor volumes at weeks 2 and 3 after treatment initiation, respectively. Thus, there was a discernible impact from PGD treatment on slowing the growth rate of MDA-MB-231 tumor volumes as compared to PTX treatment, more so than anticipated from the *in vitro* cell culture system. Gains in active targeting by the PGD seem to be amplified due to enhanced permeation and retention effects of nanoparticles observed under physiological conditions. With an improved and sustained treatment schedule along with higher drug delivery, it is anticipated that further gains in tumor growth reduction are possible.

This research, thus, provides a detailed account of the synthesis and initial biological exploration of an active-targeting, PTX-laden prodrug. Future studies, however, must overcome a few limitations of the current work. While a correlation was established in this work between *in vitro* increased cytotoxicity by PGD and cathepsin B expression, future work using enzyme

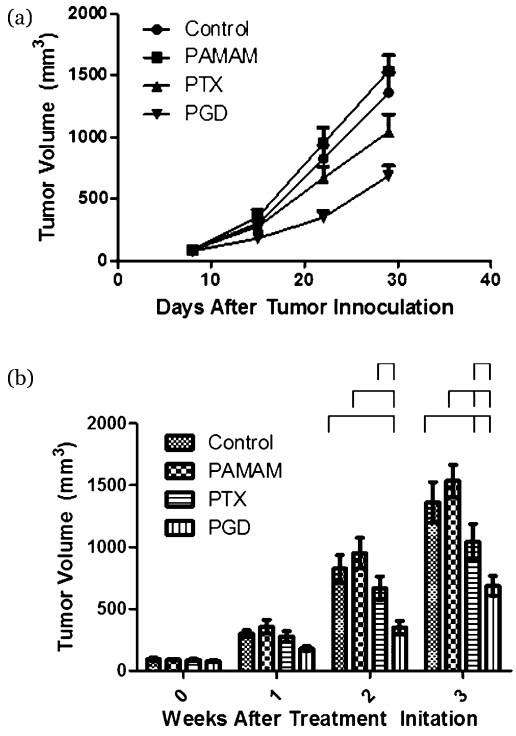

Figure 8. Effect of PGD dendrimer on human breast cancer (MDA-MB-231) xenograft tumors in mice. Subcutaneous tumors were generated by injecting 2×10^6 cells into the mammary fatpads of nude mice. When tumor volumes reached 90 mm^3, therapy was initiated and administered every other day for three intraperitoneal injections total using the following treatments: control (saline), PAMAM, PTX, and PGD. Doses of 10 mg PTX/kg body weight were administered as PTX alone or PTX-equivalent PGD. Tumor volumes were measured 1, 2, and 3 weeks after therapy initiation and reported as mean ± standard error of the mean ($n = 7$). Statistically significant results are indicated by grouped lines ($p < 0.05$). Results are reported as two different representations (a,b) of the same data set.

inhibitors may explore if increased cathepsin B expression alone is directly involved in the release of paclitaxel and inducement of cell death. As this work demonstrates, enzymes with similar structural activity to cathepsin B (such as those belonging to the papain family of enzymes) can effectively release PTX−GFLG product. Such enzymes may have concurrent over-expression with cathepsin B in malignant cancer cells; therefore, cathepsin B expression alone may not be responsible for the appreciable PGD induced cytotoxicity. Similarly, the current work provided only limited investigation into the mode of action of PGD activity on cells (whether PTX-dependent or PTX-independent), absorption kinetics, and other rationales for cell line variability in response to PGD above a certain cathepsin B expression threshold. Future work should mechanistically explore the nature of PGD activity. Finally, the *in vivo* activity in this study was limited to investigation of tumor reduction capabilities of PGD as compared to PTX. Future studies would expand on this work to probe the pharmacodynamics and distribution of PGD *in vivo* as it compares to PTX alone.

■ CONCLUSIONS

A novel PTX conjugate of PAMAM dendrimer through a cathepsin B cleavable GFLG peptide spacer (PGD) was synthesized and characterized. PTX when delivered through

this conjugate showed a better ability to reduce metabolic activity (increased cytotoxicity) to an array of cancer cells than when delivered as drug alone, in line with moderate-to-high cathepsin B expression and activity in these cells. By contrast, cells with low cathepsin B activity demonstrated the opposite relationship. Cytotoxicity by the PGD conjugate was inducted by the apoptotic pathway, similar to that of PTX treatment. The PGD conjugate demonstrated markedly higher tumor reduction in MDA-MB-231 xenograft mice models as compared to PTX treatment alone, suggesting the successful development of a cancer-specific active targeting delivery vehicle.

■ AUTHOR INFORMATION

Corresponding Author

*(A.S.) E-mail: arpsatsangi@gmail.com.

Notes

The authors declare no competing financial interest.

■ ACKNOWLEDGMENTS

Support for this research was provided, in part, by the Translational Science Training (TST) Across Disciplines program at the University of Texas Health Science Center at San Antonio, funded by the University of Texas System's Graduate Programs Initiative. The laboratory space and facilities were provided by the Department of Biomedical Engineering at the University of Texas at San Antonio, by the Department of Obstetrics and Gynecology at the University of Texas Health Science Center at San Antonio and by RANN Research Corporation, San Antonio, Texas.

■ REFERENCES

(1) American Cancer Society. Cancer Facts and Figures 2013. http://www.cancer.org/research/cancerfactsstatistics/cancerfactsfigures2013/index (accessed May 20, 2013).

(2) National Cancer Institute. Common Cancers Type. http://www.cancer.gov/cancertopics/types/commoncancers (accessed May 20, 2013).

(3) Piccart-Gebhart, M. J.; Burzykowski, T.; Buyse, M.; Sledge, G.; Carmichael, J.; Lück, H. J.; Mackey, J. R.; Nabholtz, J. M.; Paridaens, R.; Biganzoli, L.; Jassem, J.; Bontenbal, M.; Bonneterre, J.; Chan, S.; Basaran, G. A.; Therasse, P. Taxanes alone or in combination with anthracyclines as first-line therapy of patients with metastatic breast cancer. *J. Clin. Oncol.* **2008**, *26* (12), 1980−1986.

(4) Fauzee, N. J. S.; Dong, Z.; Wang, Y. L. Taxanes: Promising Anti-Cancer Drugs. *Asian Pacific J. Cancer Prevent.* **2011**, *12*, 837−851.

(5) Sparano, J. A.; Wang, M.; Martino, S.; Jones, V.; Perez, E. A.; Saphner, T.; Wolff, A. C.; Sledge, G. W.; Wood, W. C.; Davidson, N. E. Weekly paclitaxel in the adjuvant treatment of breast cancer. *New Engl. J. Med.* **2008**, *358*, 1663−1671.

(6) Singla, A. K.; Garg, A.; Aggarwal, D. Paclitaxel and its formulations. *Int. J. Pharm.* **2002**, *235*, 179−192.

(7) Holmes, F. A.; Walters, R. S.; Theriault, R. L.; Forman, A. D.; Newton, L. K.; Raber, M. N.; Buzdar, A. U.; Frye, D. K.; Hortobagyi, G. N. Phase II trial of taxol, an active drug in the treatment of metastatic breast cancer. *J. Natl. Cancer Inst.* **1991**, *83*, 1797−1805.

(8) Straubinger, R. M. Biopharmaceutics of paclitaxel (Taxol): formulation, activity and pharmacokinetics. In *Taxol: Science and Applications*; Suffness, M., Ed.; CRC Press: Boca Raton, FL, 1995; pp 237−258.

(9) Couvreur, P.; Tulkens, P.; Roland, M.; Trouet, A.; Speiser, P. Nanocapsules: a new type of lysosomotropic carrier. *FEBS Lett.* **1977**, *84* (2), 323−326.

(10) Couvreur, P.; Kante, B.; Lenaerts, V.; Scailteur, V.; Roland, M.; Speiser, P. Tissue distribution of antitumor drugs associated with polyalkylcyanoacrylate nanoparticles. *J. Pharm. Sci.* **1980**, *69* (2), 199−202.

(11) Bristol-Myers Squibb. Taxol (paclitaxel) Injection (patient information included). http://packageinserts.bms.com/pi/pi_taxol.pdf (accessed May 25, 2013).

(12) Merisko-Liversidge, E.; Sarpotdar, P.; Bruno, J.; Hajj, S.; Wei, L.; Peltier, N.; Rake, J.; Shaw, J. M.; Pugh, S.; Polin, L.; Jones, J.; Corbett, T.; Cooper, E.; Liversidge, G. G. Formulation and antitumor activity evaluation of nanocrystalline suspensions of poorly soluble anticancer drugs. *Pharm. Res.* **1996**, *13* (2), 272−278.

(13) Constantinides, P. P.; Lambert, K. J.; Tustian, A. K.; Schneider, B.; Lalji, S.; Ma, W.; Wentzel, B.; Kessler, D.; Worah, D.; Quay, S. C. Formulation development and antitumor activity of a filter sterilizable emulsion of paclitaxel. *Pharm. Res.* **2000**, *17* (2), 175−182.

(14) Weiss, R. B.; Donehower, R. C.; Wiernik, P. H.; Ohnuma, T.; Gralla, R. L.; Trump, D.; Baker, J. R.; VanEcho, D. A.; VonHoff, D. D.; Leyland-Jones, B. Hypersensitivity reactions from taxol. *J. Clin. Oncol.* **1990**, *8*, 1263−1268.

(15) Surapaneni, M. S.; Das, S. K.; Das, N. G. Designing paclitaxel drug delivery systems aimed at improved patient outcomes: Current status and challenges. *ISRN Pharmacol.* **2012**, No. 623139.

(16) Sohn, J. S.; Jin, J. I.; Hess, M.; Jo, B. W. Polymer prodrug approaches applied to paclitaxel. *Polym. Chem.* **2010**, *1*, 778−792.

(17) Sigma-Aldrich. Solubility Properties of PAMAM Dendrimers. http://www.sigmaaldrich.com/materials-science/nanomaterials/dendrimers/solubility.html (accessed May 28, 2013).

(18) Rolland, O.; Turrin, C. O.; Caminade, A. M.; Majoral, J. P. Dendrimers and nanomedicine: multivalency in action. *New J. Chem.* **2009**, *33*, 1809−1824.

(19) Nanjwade, B. K.; Bechra, H. M.; Derkar, G. K.; Manvi, F. V.; Nanjwade, V. K. Dendrimers: Emerging polymers for drug-delivery systems. *Eur. J. Pharm. Sci.* **2009**, *38*, 185−196.

(20) Tomalia, D. A.; Christensen, J. B.; Boas, U. (2012) The Dendridic State. In *Dendrimers, Dendrons, and Dendridic Polymers: Discovery, Applications and Future*; Cambridge University Press, Cambridge, UK, 2012; pp 92−95.

(21) Teow, H. M.; Zhou, Z.; Najlah, M.; Yusof, S. R.; Abbott, N. J.; D'Emanuelea, A. Delivery of paclitaxel across cellular barriers using a dendrimer-based nanocarrier. *Int. J. Pharm.* **2013**, *441*, 701−711.

(22) Wang, T. H.; Wang, H. S.; Soong, Y. K. Paclitaxel-induced cell death: Where the cell cycle and apoptosis come together. *Cancer* **2000**, *88* (11), 2619−2628.

(23) Luo, Y.; Ziebell, M. R.; Prestwich, G. D. A hyaluronic acid-taxol antitumor bioconjugate targeted to cancer cells. *Biomacromolecules* **2000**, *1* (2), 208−218.

(24) Gelderblom, H.; Verweij, J.; Nooter, K.; Sparreboom, V. Cremophor EL the drawbacks and advantages of vehicle selection for drug formulation. *Eur. J. Cancer.* **2001**, *37*, 1590−1598.

(25) Gao, Z.; Lukyanov, A. N.; Singhal, A.; Torchilin, V. P. Diacyllipid-polymer micelles as nanocarriers for poorly soluble anticancer drugs. *Nano Lett.* **2002**, *2* (9), 979−982.

(26) Liu, C.; Strobl, J. S.; Bane, S.; Schilling, J. K.; McCracken, M.; Chatterjee, S. K.; Rahim-Bata, R.; Kingston, D. G. I. Design, synthesis, and bioactivities of steroid-linked taxol analogues as potential targeted drugs for prostate and breast cancer. *J. Nat. Prod.* **2004**, *67* (2), 152−159.

(27) Hayashi, Y.; Skwarczynski, M.; Hamada, Y.; Sohma, Y.; Kimura, T.; Kiso, Y. A. Novel approach of water-soluble paclitaxel prodrug with no auxiliary and no byproduct: Design and synthesis of isotaxel. *J. Med. Chem.* **2003**, *46* (18), 3782−3784.

(28) Elliott, E.; Sloane, B. F. The cysteine protease cathepsin B in cancer. *Perspect. Drug Discovery Des.* **1996**, *6*, 12−32.

(29) Mohamed, M. M.; Sloane, B. F. Cysteine cathepsins: multifunctional enzymes in cancer. *Nat. Rev. Cancer.* **2006**, *6*, 764−775.

(30) Nouh, M. A.; Mohamed, M. M.; El-Shinawi, M.; Shaalan, M. A.; Cavallo-Medved, D.; Khaled, H. M.; Sloane, B. F. Cathepsin B a potential prognostic marker for inflammatory breast cancer. *J. Transl. Med.* **2011**, *9*, 1.

(31) Bremer, C.; Tung, C. H.; Bogdanov, A.; Weissleder, R. Imaging of differential protease expression in breast cancers for detection of aggressive tumor phenotypes. *Radiology* **2002**, *222* (3), 814−818.
(32) Dubowchik, G. M.; Firestone, R. A.; Padilla, L.; Willner, D.; Hofstead, S. J.; Mosure, K.; Knipe, J. O.; Lasch, S. J.; Trail, P. A. Cathepsin B-labile dipeptide linkers for lysosomal release of doxorubicin from internalizing immunoconjugates: Model studies of enzymatic drug release and antigen-specific in vitro anticancer activity. *Bioconjugate Chem.* **2002**, *13*, 855−869.
(33) Malugin, A.; Kopeckova, P.; Kopecek, J. Liberation of doxorubicin from hpma copolymer conjugate is essential for the induction of cell cycle arrest and nuclear fragmentation in ovarian carcinoma cells. *J. Controlled Release* **2007**, *124*, 6−10.
(34) Kurtoglu, Y. E.; Mishra, M. K.; Kannan, S.; Kannan, R. M. Drug release characteristics of PAMAM dendrimer−drug conjugates with different linkers. *Int. J. Pharm.* **2010**, *384*, 189−194.
(35) Borgman, M. P.; Ray, A.; Kolhatkar, R. B.; Sausville, E. A.; Burger, A. M.; Ghandehari, H. Targetable HPMA copolymer−aminohexylgeldanamycin conjugates for prostate cancer therapy. *Pharm. Res.* **2009**, *26* (6), 1407−1418.
(36) Duncan, R. The dawning era of polymer therapeutics. *Nat. Rev. Drug Discovery* **2003**, *2*, 347−360.
(37) Kopecek, J.; Kopeckova, P.; Minko, T.; Lu, Z. R. HPMA copolymer−anticancer drug conjugates: design, activity, and mechanism of action. *Eur. J. Pharm. Biopharm.* **2000**, *50*, 61−81.
(38) Majoros, I. J.; Myc, A.; Thomas, T.; Mehta, C. B.; Baker, J. R. PAMAM dendrimer-based multifunctional conjugate for cancer therapy: synthesis, characterization, and functionality. *Biomacromolecules* **2006**, *7* (2), 572−9.
(39) Deutsch, H. M.; Glinski, J. A.; Hernandez, M.; Haugwitz, R. D.; Narayanan, V. L.; Suffness, M.; Zalkow, L. H. Synthesis of congeners and prodrugs. 3. Water-soluble prodrugs of taxol with potent antitumor activity. *J. Med. Chem.* **1989**, *32* (4), 788−792.
(40) Ryppa, C.; Mann-Steinberg, H.; Biniossek, M. L.; Satchi-Fainaro, R.; Kratz, F. In vitro and in vivo evaluation of a paclitaxel conjugate with the divalent peptide E-[c(RGDfK)2] that targets integrin $\alpha v\beta 3$. *Int. J. Pharm.* **2009**, *368*, 89−97.
(41) Yang, N.; Ye, Z.; Li, F.; Mahato, R. I. HPMA polymer-based site-specific delivery of oligonucleotides to hepatic stellate cells. *Bioconjugate Chem.* **2009**, *20* (2), 213−221.
(42) Zhou, Y.; Yang, J.; Kopeček, J. Selective inhibitory effect of HPMA copolymer-cyclopamine conjugate on prostate cancer stem cells. *Biomaterials* **2012**, *33* (6), 1863−72.
(43) Vadlamudi, R. K.; Wang, R. A.; Mazumdar, A.; Kim, Y. S.; Shin, J.; Sahin, A.; Kumar, R. Molecular cloning and characterization of PELP1, a novel human coregulator of estrogen receptor a. *J. Biol. Chem.* **2001**, *276*, 38272−38279.
(44) Khandare, J.; Minko, T. Polymer−drug conjugates: Progress in polymeric prodrugs. *Prog. Polym. Sci.* **2006**, *31*, 359−397.
(45) Vaidya, A. A.; Lele, B. S.; Kulkarni, M. G.; Mashelkar, R. A. Enhancing ligand-protein binding in affinity thermoprecipitation: elucidation of spacer effects. *Biotechnol. Bioeng.* **1999**, *64*, 418−25.
(46) Kingston, D. G. I. Taxol: the chemistry and structure-activity relationships of a novel anticancer agent. *Trends Biotechnol.* **1994**, *12*, 222−227.
(47) Skwarczynski, M.; Hayashi, Y.; Kiso, Y. Paclitaxel prodrugs: Toward smarter delivery of anticancer agents. *J. Med. Chem.* **2006**, *49* (25), 7253−7269.
(48) Mortier, K. A.; Zhang, G.-F.; Van Peteghem, C. H.; Lambert, W. E. Adduct formation in quantitative bioanalysis: Effect of ionization conditions on paclitaxel. *J. Am. Soc. Mass Spectrom.* **2004**, *15*, 585−592.
(49) Hou, L.; Yao, J.; Zhou, J. Simultaneous LC−MS analysis of paclitaxel and retinoic acid in plasma and tissues from tumor-bearing mice. *Chromatographia* **2011**, *73*, 471−480.
(50) Erhan, Y.; Özdemir, N.; Zekioglu, O.; Nart, D.; Ciris, M. Breast carcinomas with choriocarcinomatous features: Case reports and review of the literature. *Breast J.* **2002**, *8* (4), 244−248.
(51) Filho, O. G.; Miiji, L. N. O.; Vainchenker, M.; Gordan, Â. N. Breast cancer with choriocarcinomatous and neuroendocrine features. *Sao Paulo Med. J.* **2001**, *119* (4), 154−155.
(52) L'Azou, B.; Jorly, J.; On, D.; Sellier, E.; Moisan, F.; Fleury-Feith, J.; Cambar, J.; Brochard, P.; Ohayon-Courtès, C. In vitro effects of nanoparticles on renal cells. *Part. Fibre Toxicol.* **2008**, *5*, 22.
(53) Kaczirek, K.; Schindl, M.; Weinhäusel, A.; Scheuba, C.; Passler, C.; Prager, G.; Raderer, M.; Hamilton, G.; Mittlböck, M.; Siegl, V.; Pfragner, R.; Niederle, B. Cytotoxic activity of camptothecin and paclitaxel in newly established continuous human medullary thyroid carcinoma cell lines. *J. Clin. Endocrinol. Metab.* **2004**, *89* (5), 2397−2401.
(54) Awasthi, N.; Zhang, C.; Schwarz, A. M.; Hinz, S.; Wang, C.; Williams, N. S.; Schwarz, M. A.; Schwarz, R. E. Comparative benefits of Nab-paclitaxel over gemcitabine or polysorbate-based docetaxel in experimental pancreatic cancer. *Carcinogenesis* **2013**, *34* (10), 2361−2369.
(55) GraphPad. http://www.graphpad.com/support/faqid/1566/ (accessed June 2013).
(56) Keenan, J.; Liang, Y.; Clynes, M. Two-deoxyglucose as an anti-metabolite in human carcinoma cell line RPMI-2650 and drug-resistant variants. *Anticancer Res.* **2004**, *24*, 433−440.
(57) Ashikaga, T.; Yoshida, Y.; Hirota, M.; Yoneyama, K.; Itagaki, H.; Sakaguchi, H.; Miyazawa, M.; Ito, Y.; Suzuki, H.; Toyoda, H. Development of an in vitro skin sensitization test using human cell lines: The human cell line activation Test (h-CLAT) I. Optimization of the h-CLAT protocol. *Toxicol. In Vitro* **2006**, *20*, 767−773.
(58) Zhang, X.; Stecklein, S.; Behbod, F.; Cohen, M. S. *A New Mechanism Of Action For Withaferin A In Breast Cancer: Induction Of Proteasomal-degradation of Notch1 and Notch3 Proteins*; 7th Annual Academic Surgical Congress, 2012; Control # ASC20120846.
(59) Gondi, C. S.; Rao, J. S. Cathepsin B as a cancer target. *Expert Opin. Ther. Targets* **2013**, *17* (3), 281−91.
(60) Kominami, E.; Tsukahara, T.; Bando, Y.; Katunuma, N. Distribution of cathepsins B and H in rat tissues and peripheral blood cells. *J. Biochem.* **1985**, *98* (1), 87−93.
(61) Cline, E. N.; Li, M. H.; Choi, S. K.; Herbstman, J. F.; Kaul, N.; Meyhöfer, E.; Skiniotis, G.; Baker, J. R.; Larson, R. G.; Walter, N. G. Paclitaxel-conjugated PAMAM dendrimers adversely affect microtubule structure through two independent modes of action. *Biomacromolecules* **2013**, *14* (3), 654−64.
(62) Lacroix, M.; Leclercq, G. Relevance of breast cancer cell lines as models for breast tumours: an update. *Breast Cancer Res. Treat.* **2004**, *83* (3), 249−89.
(63) Nakayama, S.; Torikoshi, Y.; Takahashi, T.; Yoshida, T.; Sudo, T.; Matsushima, T.; Kawasaki, Y.; Katayama, A.; Gohda, K.; Hortobagyi, G. N.; Noguchi, S.; Sakai, T.; Ishihara, H.; Ueno, N. T. Prediction of paclitaxel sensitivity by CDK1 and CDK2 activity in human breast cancer cells. *Breast Cancer Res.* **2009**, *11*, R12.
(64) Lee, J.; Lilly, G. D.; Doty, R. C.; Podsiadlo, P.; Kotov, N. A. In vitro toxicity testing of nanoparticles in 3D cell culture. *Small* **2009**, *5* (10), 1213−21.
(65) Sayes, C. M.; Reed, K. L.; Warheit, D. B. Assessing toxicity of fine and nanoparticles: comparing in vitro measurements to in vivo pulmonary toxicity profiles. *Toxicol. Sci.* **2007**, *97* (1), 163−80.